Technical Report

Department of Computer Science
and Engineering
University of Minnesota
4-192 Keller Hall
200 Union Street SE
Minneapolis, MN 55455-0159 USA

TR 17-004

Aerial Radio-based Telemetry for Tracking Wildlife

Haluk Bayram, Nikolaos Stefas, Volkan Isler

April 10, 2017

Aerial Radio-based Telemetry for Tracking Wildlife

Haluk Bayram, Nikolaos Stefas, Volkan Isler

Abstract This paper considers the problem of choosing measurement locations of an aerial robot in an online manner in order to localize an animal with a radio collar. The aerial robot has a commercial, low-cost antenna and USB receiver to capture the signal. It uses its own movement to obtain a bearing measurement. The uncertainty in these measurements is assumed to be bounded and represented as wedges. The measurements are then merged by intersecting the wedges. The localization uncertainty is quantified by the area of the resulting intersection. The goal is to reduce the localization uncertainty to a value below a given threshold in minimum time. We present an online strategy to choose measurement locations during execution based on previous readings and analyze its performance with competitive analysis. We also validate the strategy in simulations and in field experiments over a 5 hectare area using an autonomous aerial robot equipped with a directional antenna.

1 Introduction

Aerial robots are finding increasing use in challenging problems such as surveillance, target tracking and localization, and package delivery. In this paper, we focus on an environmental monitoring application where the goal is to localize radio-tagged animals using an autonomous Uninhabited Aerial Vehicle (UAV) as illustrated in Figure 1(a). Wildlife biologists frequently resort to radio-tagging as a tool for research and management of wildlife, where they attach a radio transmitter to an animal to be tracked and localized. The tags can be put on a collar for large animals such as moose, wolves or bears.

The authors are with the Department of Computer Science & Engineering, University of Minnesota, Minneapolis, USA. This work was supported by National Science Foundation Awards #1111638 and #1525045. The authors would like to thank Professor Forest Isbell and Dr. Mark Ditmer for providing the VHF collars, and Cedar Creek Ecosystem Science Reserve for allowing us to do the field experiments at Cedar Creek. e-mail: {hbayram, stefa125, isler}@umn.edu

The most basic and common collar is essentially a radio device which broadcasts a Very High Frequency (VHF) radio signal. There are more sophisticated collars equipped with GPS, SMS and/or satellite communication capabilities. These are usually heavy (which limits their use to only large animals) and expensive (which limits adoption). Therefore we focus on VHF collars which have been used for 55 years. Compared to other types of collars, they are low cost, have reasonable accuracy, and 5-6 times longer life time [8]. Because of the longevity of VHF collars, the physical interaction with collared animals is minimized, which also decreases the possibility of abandonment of collared animals by its mother or group members. On the other hand, manually tracking animals with VHF collars is labor-intensive. In

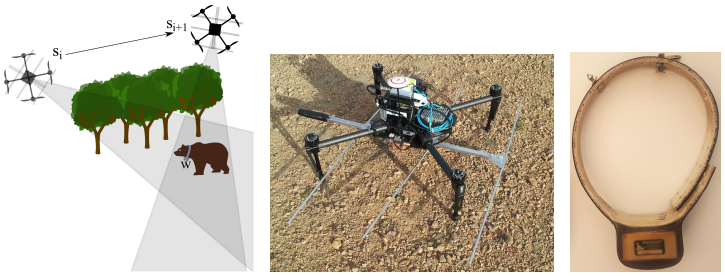

(a) (b) (c)

Fig. 1 (a) The Online Target Localization Problem: A collared animal is to be localized. The goal is to minimize the time spent in localizing the target in such a way that the localization uncertainty is below a desired level. In the figure, the UAV is moving from s_i to s_{i+1} to take the next bearing measurement. The localization is done by intersecting the bearing measurements. The uncertainty is a function of the measurement locations relative to the (unknown) target location. (b) The quadrotor with an on-board computer, USB receiver and 3-element Yagi antenna. (c) The collar (VHF transmitter operating at 163.739 MHz) used for the radio-tracking of animals.

order to estimate the position of the collared animal, various types of ground-based techniques have been used. These include homing in on the animal, triangulation, fixed towers, and vehicle mounted antenna [7]. The first two techniques are cost-effective, but labor-intensive. The other two require construction and are usually costly. In the homing technique, researchers rely on the fact that signal strength decreases as distance increases. Therefore, they follow the gradient of the signal to get to the animal. This method does not always work because estimating the gradient is difficult due to multi-path effect and interference from the ground or the environment. Often the directionality of the signal is also used. By rotating the antenna, a coarse bearing measurement is obtained. In the triangulation technique, two or more bearing measurements are merged to localize the animal. Depending on the measurement noise, triangulation performance relies highly on where the bearing measurements are taken and how far they are from the target. In both techniques, walking from one measurement location to another location may take long time. During that time, the animal can move, which results in bad localization perfor-

mance. UAVs can make the tracking process more accurate and faster especially when the animal's living area is not easily accessible to humans. In this paper, we present a system capable of localizing collared animals.

When a directional antenna is used for VHF radio-tracking, bearing information is more reliable than range information because the range information is too sensitive to signal characteristics. When there is a small change in these characteristics due to e.g. the line of sight and weather, the range inference becomes unreliable. However, since bearing is determined by the direction where the signal strength is the strongest, it is not affected by these changes. Hence, our approach is based on bearing measurements. In [11], an EKF-based online algorithm is proposed to localize radio-tagged fish using ambiguous bearing measurements, comparing it with optimal offline strategy. However, the approach requires a rough initial estimate and noise model. The system is based on ground and surface vehicles. Here we focus on a UAV-based system. The work in [3] uses a two-point phased array antenna and custom designed circuitry for signal capturing in order to collect bearing measurements with an aerial robot. The authors present a strategy for choosing measurement so as to improve localization uncertainty to within 50 meters without providing any guarantee on the localization. Our system uses an off-the-shelf antenna and signal receiver, and our bearing strategy provides accuracy guarantees and better localization performance.

Our contributions can be summarized as follows: we present (i) an online algorithm to locate a target using bounded bearing measurements along with a cost analysis of the algorithm, (ii) implementation of the algorithm on a quadrotor to localize a VHF collar which is then validated in field experiments.

2 System Description

Our system consists of an aerial robot with an on-board computer and sensors (GPS, IMU, compass), and radio-tracking components (signal receiver, directional antenna and a radio transmitter collar attached to the animal).

The aerial robot used in this work is a quadrotor DJI Matrice 100. It has a takeoff weight of 3.4 kg, flies for approximately 25 minutes with two batteries and travels at speeds of up to 17 m/s with a payload of 1 kg. The onboard processor is an NVIDIA Jetson TX1 computer with an Ubuntu 14.04 Linux operating system and ROS-based framework. The ROS (Robot Operating System) middleware allows the integration of our various components into the system. All processing is performed online with the on-board computer. A WiFi module enables communication with a ground stationed laptop computer, which is used only for observing the status of the UAV. Autonomous GPS waypoint navigation with ROS-based integration is provided by the manufacturer with a hovering accuracy of 2.5 meters. The developed online algorithm was implemented as a ROS node on this framework.

As shown in Figure 1(b), the UAV has a 3-element Yagi antenna mounted underneath. The antenna is connected to an inexpensive RTL-SDR (Software Defined

Radio) USB receiver, which is tunned to the collar's frequency [12]. The signal captured by the USB receiver is read in IQ data format through `rtl_sdr` software[1], which is an IQ recorder for RTL2832 based DVB-T receivers.

The target is tagged with a collar, which is a Telonics MOD-500 VHF radio transmitter operating at the pre-set frequency 163.739 MHz (Figure 1(c)). The collar transmits 80 pulses with width of 15 msec in active mode and 40 pulses per minute in inactive mode, respectively.

3 Preliminaries

3.1 Sensing Model & Uncertainty Measure

We consider bearing measurements with bounded noise. The bounded noise model is advantageous over probabilistic models when there is no precise sensor model [5, 10]. In this model, the sensor provides a bearing corrupted with a bounded noise α as shown in Figure 2(a). The angle difference ϕ between the true bearing and measured bearing is at worst α. The 2D wedge yielded by a measurement is guaranteed to contain the target.

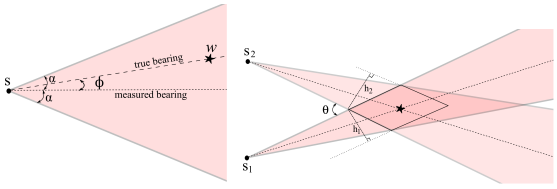

(a) (b)

Fig. 2 (a) Sensing model. The target is located at w and known to lie in the measurement wedge. The true bearing is corrupted with unknown but bounded noise α. (b) Approximating the intersection of two measurements as a parallelogram. The target location w is denoted by star.

The localization process is basically done by intersecting measurements taken so far. The resulting intersection is considered the location uncertainty. The intersection of two bearing measurements can be seen in Figure 2(b) in which the dark shaded area denotes the area where the target lies in. The mathematical representation of the intersection gets more complicated when the number of measurements increases. We can make a simplification by approximating the resulting intersection as a parallelogram. So, the localization uncertainty U for two measurements taken from locations s_1 and s_2 for a target at location w can be given as the area of this parallelogram [2]:

$$U(s_1,s_2,w) = \frac{h_1 h_2}{|sin\theta|} \approx \frac{(2d(s_1,w)tan\alpha)(2d(s_2,w)tan\alpha)}{|sin\theta|} = (2tan\alpha)^2 \frac{d(s_1,w)d(s_2,w)}{|sin\theta|} \quad (1)$$

[1] `rtl_sdr` software is available at http://osmocom.org/projects/sdr/wiki/rtl-sdr

where the notation $d(a,b)$ denotes the Euclidean distance between points a and b. The term $(2tan\alpha)^2$ in Equation 1 does not depend on the target-sensor geometry. The rest of the equation is similar to the geometric dilution of precision (GDOP) [6], which is commonly used to measure the uncertainty in estimating the location of a target from two bearing measurements.

3.2 Problem Statement

Let the true target location be denoted by w. The robot can take bearing measurements of the target location. Each bearing measurement yields a bounded wedge with angular clearance 2α such that the wedge will contain the target. The localization of the target is performed by intersecting the wedges obtained from bearing measurements. Each measurement requires a fixed amount of time τ_m. Measurement locations are denoted by s_i for measurement i. The full sequence of N measurements is $S = \{s_1, \ldots, s_N\}$.

The problem is to determine measurement locations s_i in an online manner so as to localize a target to a desired localization uncertainty $U^\star$ such that the following cost for the localization will be minimized

$$cost(S) = \sum_{i=1}^{N-1} d(s_i, s_{i+1})/v + N\tau_m \tag{2}$$

While the first term in Equation 2 shows the time spent in traveling to each measurement locations, the second term corresponds to the total measurement time. For the sake of notational simplicity, the robot is assumed to move at a unit velocity, hence the velocity term v is dropped from the cost function.

4 Online Target Localization

In evaluating the performance of an online algorithm, an optimal offline strategy with full information is commonly used. The ratio between the cost of online strategy and the optimal offline strategy is called competitive ratio, which provides an upper bound for how large the cost of the online algorithm can be with respect to the optimal offline strategy. So, we will first derive a lower bound for an offline strategy in order to compute the competitive ratio for the online strategy.

4.1 Optimal Offline Strategy

We begin by deriving a lower bound on the time required to localize the target when the optimal measurement sequence is used. This sequence is planned in an offline manner with knowledge of the true target location w.

In order to obtain a finite intersection area, at least two measurements need to be taken from two different locations which are not collinear with the target. Therefore, the optimal offline strategy takes at least two measurements.

Proposition 1. *Suppose the first measurement is taken from s_1 and the uncertainty in estimating the target's location is desired to be at most $U^\star$. Suppose the second measurement s_2 is taken at (x,y) and the target is located at $(0,0)$. Using the uncertainty measure in Equation 1, the locus of all such (x,y) is defined by $x^2 + \left(y \pm \frac{C}{2d(s_1,w)}\right)^2 \leq \left(\frac{C}{2d(s_1,w)}\right)^2$ where $C = \frac{U^\star}{(2tan\alpha)^2}$.*

This inequality is the mathematical expression of the **measurement region** for the next measurement s_2, which represents two disks with radius $\frac{C}{2d(s_1,w)} = \frac{U^\star}{2(2tan\alpha)^2 d(s_1,w)}$ as shown in Figure 3(a).

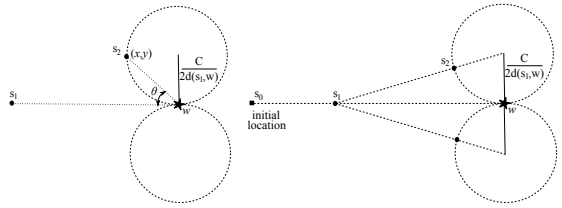

Fig. 3 (a) The measurement region of the second measurement is defined by a disk with radius $\frac{C}{2d(s_1,w)}$ centered at $(0,\pm\frac{C}{2d(s_1,w)})$. The target is known to be at location w. The first measurement is taken from s_1. The second measurement can be taken from the measurement region shown by the dashed circles in order to satisfy the desired uncertainty $U^\star$. (b) Optimal measurement locations. The robot moves from the initial location s_0 to s_1 in order to take its first measurement. Then, the second measurement is taken at the closest point s_2 on the disk to the first measurement location s_1.

The work in [4] uses a similar derivation for the locus of the next measurement based on the Fisher Information Matrix. However, our uncertainty measure and derivation are only based on geometry.

In Proposition 1, we assume that the initial location of the robot coincides with the initial measurement. In the offline case where the target location is known, this choice for the first measurement may lead to a suboptimal solution. In order to rectify this, the robot moves a certain distance towards the target, then takes the first measurement as illustrated in Figure 3(b). Then, it moves to the nearest location at

the locus where it takes the second measurement. Following this strategy will cost less in terms of distance traveled.

Theorem 1. *Suppose the robot is initially at s_0 and the target is located at w. The cost of the optimal offline solution $OPT = OPT_d + OPT_m$ is lower bounded by $d(s_0, w) - (\sqrt{2}-1)\sqrt{C} + 2\tau_m$.*

4.2 Target On a Line

First, we will consider the case where we would like to localize a target on a known line. We adapt a doubling strategy commonly used for solving online problems such as the lost-cow problem [1].

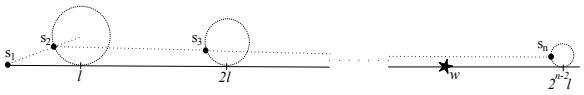

Fig. 4 The measurement locations $\{s_1, \ldots, s_n\}$ computed by the online algorithm applying the doubling strategy in the case where the target is known to be on the line. The dashed circles represent the measurement regions for the corresponding measurements.

In the online algorithm proposed here to localize a target on a known line, the measurement locations are determined in such a way that the possible target locations are hypothesized to be at doubling distances away from the initial location. The next measurement location is determined based on the optimal offline strategy for the current hypothesis. As shown in Figure 4, after the first measurement, we can know the direction of the target on the line. To determine the second measurement location, the target is assumed to be at the location l away from the initial location. Based on this assumption, the measurement region of the second measurement is calculated using the inequality in Proposition 1. The next measurement will be the closest point at the measurement region to the previous measurement. After each measurement, if the target is not localized, its possible location is determined such that it will be further away from the previous location in a doubling manner. The robot may pass by the target without localizing it. In that case, the next measurement will give a reverse direction. After that, instead of applying the doubling strategy, the next possible target location is determined using the halving strategy. The algorithmic version of this online strategy can be seen in Algorithm 1.

Theorem 2. *Suppose the target is known to be on a known line. Given the measurement noise α, the desired localization uncertainty $U^\star$ and the minimum step length l, the online algorithm described in Algorithm 1 has a competitive ratio of*

Algorithm 1 Localizing a target on a known line

$i \leftarrow 1$ {Initialize the measurement index}
$strategy \leftarrow$ DOUBLING
Take the initial bearing measurement s_1 on the line
Determine the direction of the target dir {1 for right, -1 for left}
Initialize the distance l
$w' \leftarrow dir \times l$ {The target is assumed to be w' away from the initial measurement location on the dir side}
while $U > U^\star$ **do**
    {Keep repeating as long as the uncertainty U is higher than the desired uncertainty $U^\star$}
    $i \leftarrow i+1$
    Determine the next measurement location s_i based on the assumption that the target is w' away from s_{i-1}
    Take a bearing measurement at s_i
    if $i > 2$ and the returning condition is met **then**
        $dir \leftarrow -1 \times dir$ {Reverse the motion direction}
        $strategy \leftarrow$ HALVING
    end if
    if $strategy$ is DOUBLING **then**
        $l \leftarrow 2l$ {Apply the doubling strategy}
    else
        $l \leftarrow l/2$ {Apply the halving strategy}
    end if
    $w' \leftarrow w' + dir \times l$ {The target is assumed to be w' away from the previous location on the dir side}
    Compute the localization uncertainty U by intersecting the measurements
end while

$max\Big(\frac{\frac{3\pi}{2}L}{L-\left(\sqrt{2}-1\right)\sqrt{C}}, log_2\big(\frac{2L}{l}+2\big)\Big)$ *where L is the distance between the target and the initial location of the robot and* $C = \frac{U^\star}{(2tan\alpha)^2}$.

A sample scenario from the simulations conducted using Algorithm 1 is shown in Figure 5. After the 6th measurement, the robot realizes it passed by the target and starts applying the halving strategy. After taking the 9th measurement, the robot locates the target within the desired uncertainty.

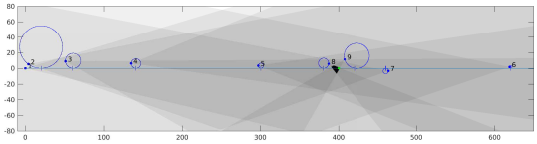

Fig. 5 A sample from the simulations where the target is known to be on the line, but its location on this line is not known. The bearing noise α is set to $\pi/12$. The ticks on the line show the assumed target locations. The disks represent the measurement region for an assumed target location. The thick dots show the measurement locations. After 9 measurements, the target is localized. The final localization uncertainty is black in color.

Theorem 2 in practice: Taking the radio-tracking of animals in wildlife into consideration, we can have practical upper bounds for the variables L, l, α and $U^\star$ in Theorem 2. VHF collars may have a range of 3-20 km on the ground. This range can be extended to 35-100 km by aerial tracking [9]. In our application, this range is about 1-2 km, hence L can be at most 2 km. The localization uncertainty area $U^\star$ can be thought of as a disk with radius $\sqrt{\frac{U^\star}{\pi}}$, which is set to 10 meters in our field experiments. We can also use this radius to set l. The bearing noise α is $\pi/6$. Given these settings, $SOL \leq 8.65OPT$, which means that the cost of the proposed online algorithm is within factor 8.65 of the optimal offline solution.

4.3 Target Localization on the Plane

Benefiting from the strategy in the online algorithm proposed for the case in which the target is on a line, we will extend the algorithm to the problem in which the target can be anywhere on a 2D environment.

In this case, we do not have any prior knowledge on the target location as opposed to the case where the target is on the line. But if the bearing noise α is small enough, we can make the assumption that the target lies on the bisector of the first measurement. Therefore, the strategy in Algorithm 1 can be applied for the target on 2D under this assumption. The validity of the assumption highly depends on how far the target is away from the initial location and the amount of the desired uncertainty, which in turn will affect the localization performance. The larger the measurement noise α is, the more the localization performance deteriorates.

Figure 6 shows a sample from the simulations where the target can be anywhere on a plane. The target can be localized due to its proximity to the bisector. However,

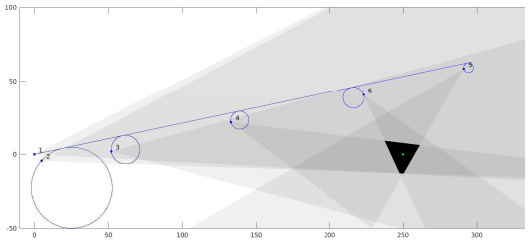

Fig. 6 A sample from the simulations where the target can be anywhere on a plane. The bearing noise α is set to $\pi/12$. The target is close enough to the bisector of the first measurement in order to localize it up to the desired uncertainty by executing Algorithm 1.

if the proximity gets larger, Algorithm 1 cannot localize the target.

We turn this insight into a new strategy by detecting this situation and resetting the strategy:

1. Take a bearing measurement
2. Execute the line strategy in Algorithm 1 with respect to the bisector of the measurement

3. If the target is not localized, go to step-1

At the onset of the mission, after taking a bearing measurement, the algorithm applies the doubling strategy by increasing i by one until the returning step $i = k$ is detected. Then, the halving strategy is applied by decreasing i by 1 until $i = 0$. The procedure described so far is what Algorithm 1 proposes. At this point, there are two possibilities: (i) the target is localized either because the assumption that the target is on the line defined by the bisector of the first measurement holds or because the desired localization uncertainty $U^\star$ is large enough to localize the target using the line strategy, (ii) the target is not localized because it is far away from the line or the desired uncertainty $U^\star$ is small. In the latter case, Algorithm 1 is restarted by assuming the target lies on the line defined by the bisector of the measurement taken when i is decreased to 0. The restarting process is repeated until the target is localized.

The analysis of the online algorithm can be divided into two cases based on the size of the measurement region generated for the offline optimal solution and whether the measurement region intersects the bisector of the first measurement:

- Case-I: The measurement region intersects the bisector and is large enough such that the bisector lies in the region, therefore there exists any measurement taken within this measurement region under the assumption that the target is on the bisector. Executing Algorithm 1 once will be sufficient to localize the target as in Figure 6.
- Case-II: Either the measurement region does not intersect the bisector or the measurement region intersects the bisector but it does not contain any measurement location generated assuming the target is on the bisector. This case requires restarting of Algorithm 1 after it fails to localize the target under the assumption that the target is on the current bisector. A sample simulation for Case-II can be seen in Figure 7(c).

Case-I is depicted in Figure 7(a). Here the offline optimal solution moves to the location s_2 on the measurement region with radius $\frac{C}{2L}$ by traveling $d(s_1,s_2) = L-(\sqrt{2}-1)\sqrt{C}$. The online strategy needs to move beyond location b, which is the intersection of the measurement region's boundary and the bisector. The distance $d(s_1,b)$ can be at most L. So the last measurement can be taken from a location which is at worst $2L$ far away from s_1. While the offline optimal solution requires only two measurements, the online strategy takes at most $n = log_2(\frac{L}{l})+1 = log_2(\frac{2L}{l})$ measurements. Hence, the costs of the optimal solution and the online strategy are as follows:

$$\begin{aligned} OPT &= OPT_d + OPT_m \geq L-(\sqrt{2}-1)\sqrt{C}+2\tau_m \\ SOL &= SOL_d + SOL_m \leq 2L + log_2(2L/l)\tau_m \\ &\leq \frac{2L}{L-(\sqrt{2}-1)\sqrt{C}} OPT_d + \frac{log_2(2L/l)}{2} OPT_m \\ &\leq max\Big(\frac{2L}{L-(\sqrt{2}-1)\sqrt{C}}, log_2(\sqrt{\frac{2L}{l}})\Big) OPT \end{aligned} \tag{3}$$

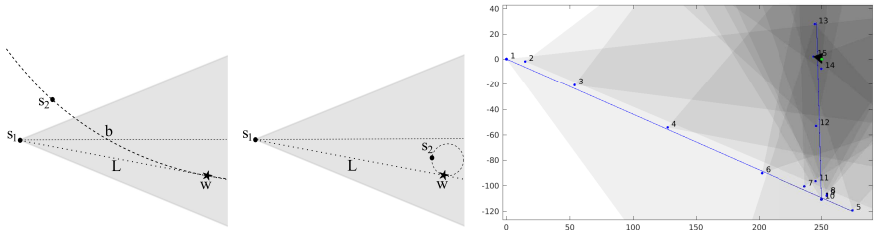

(a) Case-I (b) Case-II (c) A sample simulation for Case-II

Fig. 7 For both cases, the offline optimal solution takes the second measurement from s_2 on the measurement region. (a) In Case-I, the measurement region for the first measurement intersects the bisector of the first measurement. After the first measurement, the online algorithm determines the next measurement locations based on the assumption that the target is on the bisector. Whenever a measurement is taken within the measurement region, the target is guaranteed to be localized. (b) In Case-II, since the measurement region generated by considering the first measurement location s_1 and the target location w does not intersect the bisector of the first measurement, the online strategy first needs to realize that the target cannot be localized under the assumption that it is on the line, hence the online strategy should determine where it leaves the line. (c) A sample from the simulations for Case-II. The bearing noise α is set to $\pi/6$. The thick dots show the measurement locations. After the 15th measurement, the target is localized. The final localization uncertainty is shaded by black color.

Case-II is depicted in Figure 7(b). As in Case-I, the offline optimal solution moves to the location s_2 on the measurement region with the radius $\frac{C}{2L}$ by traveling $d(s_1,s_2) = L-(\sqrt{2}-1)\sqrt{C}$. Since the target w is not on the line or close enough to the line, the online algorithm cannot localize it just by moving on the line. After the returning condition in which the angle between the current bisector and the bearing is greater than $\pi/2$ is satisfied as shown in Figure 11(a), the online algorithm starts applying the halving strategy at the location s_κ until the index i decreases from κ to 0.

Lemma 1. *Assuming the target is on the line defined by the bisector of the first measurement, the online algorithm starts applying the halving strategy after taking at worst-case κth measurement where* $\kappa = \left\lceil log_2\left(\frac{2L}{l}sec\alpha + 2\right)\right\rceil$.

The robot leaves the line when the step index i is decreased to 0. Now it is assumed that the target is on the bisector of the measurement taken at this leaving location. How many times this process is repeated can be upper-bounded by enforcing the robot to enter into the measurement region with radius $\frac{C}{2L}$ defined by the first measurement.

Lemma 2. *To localize a target on 2D, Algorithm 1 is repeated at most γ times where* $\gamma = \frac{log_2\left(\frac{C}{2L^2}\right)}{log_2\left(tan\alpha\right)}$.

Theorem 3. *The online algorithm proposed to localize a target on 2D has a competitive ratio of* $max\left(\frac{2\gamma Lsec\alpha}{L-(\sqrt{2}-1)\sqrt{C}}, \kappa\gamma\right)$.

5 Experiments

The proposed approach was implemented on a quadrotor with a Yagi antenna as described in Section 2. First, we will describe how to take bearing measurements using the Yagi antenna and give the details of the received signal characteristics. Then the experimental setting will be presented along with the results from the field experiments.

Bearing Measurements: Yagi antennas have one direction where the signal strength is at a maximum. This happens when the shortest element of the antenna is pointed towards the collared animal. Therefore, to determine the direction of the collar, the Yagi antenna must be rotated.

To measure a target bearing, the robot rotates 360 degrees. It stops at each predefined angle increment and takes a measurement. The bearing can be determined by computing the interval with the maximum average pulse amplitude.

In order to validate this method, we first performed field experiments with a ground vehicle. The step angle for the rotation was set to 30 degrees. The robot made eleven 30-degree rotations and took 12 three-second measurements. The target was located at 0 degrees. As can be seen in the sample measurements (Figure 8), the more the antenna's direction deviates from the correct bearing, the more the measurements get corrupted. The same experiments were repeated with the UAV. It was observed that the UAV's rotors and communication system do not have any considerable effect on the bearing measurements. We also tested the effect of altitude variation on the measurements. First we placed the collar 300 meters away from the UAV, then took bearing measurements for 10, 15 and 30 meter altitudes. The higher altitude provides more reliable bearing measurements. Therefore, in the field experiments, the UAV flew at 30 meters.

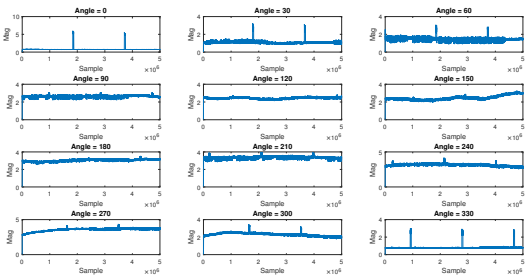

Fig. 8 Sample bearing measurements obtained by rotating the Yagi antenna. The target was located at 0 degrees. Each measurement takes 3 seconds. The plots show the magnitude of the received signal from 30-degree rotations. The measurement taken from 0 degrees has the strongest and least noisy pulses.

Field Experiments: The algorithm described in Section 4.3 was implemented on the quadrotor UAV (Figure 1(b)). The localization strategy and computation of bearing measurements were coded as a ROS node in Python so that the UAV can perform its task autonomously. All the processing is done on the UAV. The ground station is used only for observing the current state of the UAV.

The system was tested at Cedar Creek Ecosystem Science Reserve where the wildlife biologists plan to tag wolves with VHF collars this summer. The collar was deployed at a location 150 meters away from the initial location of the UAV. Based on the bearing measurement analysis, the bearing noise α was set to 30 degrees. The desired localization uncertainty $U^\star$ was set to 315 m^2, which corresponds to the area of a disk with radius 10 meters. The robot runs its localization task until the localization uncertainty is below $U^\star$. The minimum step length l was chosen as the radius of the corresponding disk of the desired localization uncertainty.

A sample field experiment is shown in Figure 9. The location of the collar is marked by "T". Each measurement is shown as a gray wedge. The UAV starts at the first measurement location M1. Until the fourth measurement, the UAV applies the doubling strategy. After that, the halving strategy is applied. After the fifth measurement, the target is localized to the desired localization uncertainty. The whole experiment took 13 minutes, for which the UAV can fly with one battery. In the field experiments, the collar was in active mode.

Fig. 9 A sample field experiment at Cedar Creek Ecosystem Science Reserve, MN. The target location is marked by "T". Each measurement is shown as a gray wedge. The UAV starts at the first measurement location M1. Until the fourth measurement, the UAV applied the doubling strategy. After that, the halving strategy was applied. After the fifth measurement, the target was localized to the desired localization uncertainty. The dark gray area is the resulting intersection of all the measurements, showing the area where the target is.

Insights from Field Experiments: In our system, the time spent in rotating the UAV around itself, recording the measurements and analyzing them to get the bearing to the target takes approximately 2.5 minutes. This is a long duration for a single bearing measurement. It can be decreased by system improvements, in particular by switching from Python to C++ for signal analysis. Furthermore, the current

measurement-taking approach requires the robot to rotate around a fixed point while capturing the signal. Instead, the UAV translation and rotation can be combined to decrease the overall travel time. We will investigate this interesting but challenging problem in our future work.

6 Conclusion

In this work, we proposed an online strategy to choose measurement locations during execution so as to localize VHF radio collared animals using an aerial robot. We showed the performance of the online strategy with competitive analysis. We also validated the strategy in field experiments using an autonomous aerial robot equipped with a directional antenna.

In the next stage, the flight time will be improved by optimizing the measurement-taking technique and the analysis of the captured signal. We would also like to revise the system design and reduce the payload by replacing heavy items with lighter ones. To achieve long-term autonomy, in case of insufficient power, the UAV will be enabled to go to a home position in order to replace (or even recharge) the battery, then resume its localization task. Our future work will also focus on extending the strategy to use multiple aerial robots. One of the main challenges in the multirobot extension is to maintain communication to exchange their measurement history.

References

1. Baieza-Yates, R.A., Culberson, J.C., Rawlins, G.J.E.: Searching with uncertainty. Tech. Rep. 239, Indiana Univeristy (1988)
2. Bamberger, R.J., Moore, J.G., Goonasekeram, R.P., Scheidt, D.H.: Autonomous geo location of rf emitters using small, unmanned platforms. Johns Hopkins APL Technical Digest **32**(3), 636–646 (2013)
3. Cliff, O., Fitch, R., Sukkarieh, S., Saunders, D., Heinsohn, R.: Online Localization of Radio-Tagged Wildlife with an Autonomous Aerial Robot System. In: Proceedings of Robotics: Science and Systems. Rome, Italy (2015)
4. Hook, J.V., Tokekar, P., Isler, V.: Algorithms for cooperative active localization of static targets with mobile bearing sensors under communication constraints. IEEE Transactions on Robotics **31**(4), 864–876 (2015)
5. Isler, V., Bajcsy, R.: The sensor selection problem for bounded uncertainty sensing models. IEEE Transactions on Automation Science and Engineering **3**(4), 372–381 (2006)
6. Kelly, A.: Precision dilution in triangulation based mobile robot position estimation. In: Proceedings of the Int. Conf. on Intelligent Autonomous Systems. Amsterdam (2003)
7. Mech, L.D.: Handbook of Animal Radio-Tracking. University of Minnesota Press (1983)
8. Mech, L.D., Barber, S.M.: A critique of wildlife radio-tracking and its use in national parks - a report to the U.S. National Park Service. Tech. rep. (2002)
9. Millspaugh, J., Marzluff, J.M.: Radio tracking and animal populations. Academic Press (2001)
10. Tokekar, P., Isler, V.: Sensor placement and selection for bearing sensors with bounded uncertainty. In: IEEE Int. Conf. on Robotics and Automation, pp. 2515–2520 (2013)

11. Vander Hook, J., Tokekar, P., Isler, V.: Cautious greedy strategy for bearing-only active localization: Analysis and field experiments. Journal of Field Robotics **31**(2), 296–318 (2014)
12. VonEhr, K., Hilaski, S., Dunne, B.E., Ward, J.: Software defined radio for direction-finding in uav wildlife tracking. In: IEEE Int. Conf. on Electro Information Technology, pp. 464–469 (2016)

7 Appendix

7.1 Proof for Proposition 1

Proof. Using the uncertainty measure in Equation 1, the locus of all such (x,y) can be calculated as follows:

$$U^\star \geq (2tan\alpha)^2 \frac{d(s_1,w)d(s_2,w)}{|sin\theta|}$$

We know the distance $d(s_1,w)$ from the first measurement s_1 to the target w. Collecting all the known quantities on one side and expressing $d(s_2,w)$ and $sin\theta$ in terms of (x,y),

$$\begin{aligned}
\frac{d(s_2,w)}{|sin\theta|} &\leq \frac{U^\star}{(2tan\alpha)^2 d(s_1,w)} \\
\frac{\sqrt{x^2+y^2}}{|y/\sqrt{x^2+y^2}|} &\leq \frac{U^\star}{(2tan\alpha)^2 d(s_1,w)} \\
x^2+y^2 &\leq \frac{U^\star}{(2tan\alpha)^2 d(s_1,w)}|y| \\
x^2+\Big(y \pm \frac{C}{2d(s_1,w)}\Big)^2 &\leq \Big(\frac{C}{2d(s_1,w)}\Big)^2
\end{aligned} \tag{4}$$

where $C = \frac{U^\star}{(2tan\alpha)^2}$. □

7.2 Proof for Theorem 1

Proof. The total traveled distance is equal to the summation of the distance from s_0 to s_1 and the distance from s_1 to the nearest point at the measurement region:

$$\big(d_0 - d_1\big) + \Big(\sqrt{d_1^2 + \Big(\frac{C}{2d_1}\Big)^2} - \frac{C}{2d_1}\Big) \tag{5}$$

Here, d_i denotes the distance $d(s_i,w)$. To obtain the minimum traveled distance, the first derivative of Equation 5 is solved for $d(s_1,w)$ given the initial distance $d(s_0,w)$. So, the distance is minimized when $d(s_1,w) = \sqrt{C/2}$. The total distance to be traveled is

$$d_0 - d_1 + d(s_1,s_2) = d_0 - \sqrt{\frac{C}{2}} + \big(\sqrt{C} - \sqrt{\frac{C}{2}}\big) = d_0 - \big(\sqrt{2}-1\big)\sqrt{C} \tag{6}$$

In order to obtain a finite intersection area, at least two measurements need to be taken from two different locations which are not collinear with the target. Therefore, the optimal offline strategy takes at least two measurements, which means $OPT_m \geq 2\tau_m$. So, the cost of the optimal offline strategy can be expressed by combining the distance and the measurement costs as:

$$OPT = OPT_d + OPT_m \geq d(s_0, w) - (\sqrt{2}-1)\sqrt{C} + 2\tau_m \tag{7}$$

which proves the theorem statement. □

7.3 Proof for Theorem 2

Proof. For analyzing Algorithm 1, we divide it into two phases: (i) doubling, and (ii) halving. Suppose the target is at distance L on the line. The target may be localized in the first phase. But we would like to compute the worst-case localization performance, which includes the halving phase as well. The worst-case depicted in Figure 10 occurs when the target is located at the location which is just ε away from the candidate location determined for nth measurement. Therefore, the distance be-

Fig. 10 The worst-case where the target is at the location a little away from the candidate target location for nth measurement.

tween the target and the initial measurement can be written in terms of the minimum step length l and the number of measurement n:

$$L = \sum_{i=0}^{n-2} 2^i l = (2^{n-1}-1)l + \varepsilon$$

which implies $n = log_2(\frac{L-\varepsilon}{l}+1)+1 \leq log_2(\frac{2L}{l}+2)$. The distance traveled to the nth measurement location can be upper bounded by the half circumference of a circle with radius $L/2$, which is $\frac{\pi}{2}L$. Because of this overshoot, the robot returns after the $(n+1)$th measurement and starts to apply the halving strategy. So, it takes at worst $2n$ measurements and travels $\frac{3\pi}{2}L$ in order to localize the target.

The total cost of the online algorithm is

$$SOL \leq \frac{3\pi}{2}L + 2log_2(\frac{2L}{l}+2)\tau_m \tag{8}$$

From Theorem 1, we know the optimal distance cost $OPT_d \geq L - \left(\sqrt{2}-1\right)\sqrt{C}$ and the optimal measurement cost $OPT_m \geq 2\tau_m$. The cost of the online algorithm is rewritten in terms of OPT_d and OPT_m as:

$$SOL \leq \frac{\frac{3\pi}{2}L}{L-\left(\sqrt{2}-1\right)\sqrt{C}}OPT_d + log_2(\frac{2L}{l}+2)OPT_m$$
$$\leq max\Big(\frac{\frac{3\pi}{2}L}{L-\left(\sqrt{2}-1\right)\sqrt{C}}, log_2(\frac{2L}{l}+2)\Big)OPT \tag{9}$$

which proves the theorem statement. □

7.4 Proof for Lemma 1

Proof. In order to determine the returning location, we make an assumption that the target w lies on the boundary of the measurement wedge, which gives the worst-case in terms of distance because the robot moves along the bisector of the first measurement and relocating the target to the boundary increases the distance to the bisector . This can be seen in Figure 11(b). The distance $d(s_1, s_\kappa)$ is equal $(2^{\kappa-1}-1)l$. We also know from Figure 11(b) that $d(s_1, s_k)$ is equal to $Lsec\alpha$. Equating these two quantities, we can calculate the required number of steps κ for the returning,

$$(2^{\kappa-1}-1)l = Lsec\alpha$$
$$\kappa \leq \Big\lceil log_2\Big(\frac{2L}{l}sec\alpha+2\Big)\Big\rceil \tag{10}$$

which proves the lemma. □

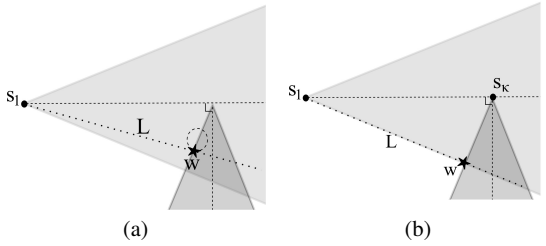

Fig. 11 (a) The returning location on the line. (b) If the target is located on the boundary of the measurement wedge, the returning location s_k will become further, which gives the worst-case.

7.5 Proof for Lemma 2

Proof. Of course, the next measurements improve the localization uncertainty, thereby enlarging the measurement region. But to have an upper-bound, we will use the measurement region generated for the first measurement as a worst-case. Let γ be the total number of leaving locations we need. If the distance between the last

leaving point and the target location is less than the radius of the measurement region generated for the first measurement location, we have sufficient measurements to localize the target:

$$L\Big(sec\alpha sin\alpha\Big)^{\gamma} \leq \frac{C}{2L}$$

From this inequality, the upper-bound for γ is found as

$$\gamma \leq \frac{log_2\big(\frac{C}{2L^2}\big)}{log_2\big(tan\alpha\big)} \tag{11}$$

which gives how many times Algorithm 1 is repeated at most. □

7.6 Proof for Theorem 3

Proof. By combining Lemma 1 and Lemma 2, we see that the distance traveled is less than $\gamma 2d(s_1,s_\kappa) = \gamma 2Lsec\alpha$ and the time spent in taking measurements becomes at most $2\kappa\gamma\tau_m$. The cost of the online algorithm is:

$$\begin{aligned} SOL &= SOL_d + SOL_m \\ &\leq \gamma 2d(s_1,s_\kappa) + 2\kappa\gamma\tau_m \end{aligned} \tag{12}$$

From Theorem 1, we know the optimal distance cost $OPT_d \geq L - \big(\sqrt{2}-1\big)\sqrt{C}$ and the optimal measurement cost $OPT_m \geq 2\tau_m$. The cost of the online algorithm is rewritten in terms of OPT_d and OPT_m as:

$$\begin{aligned} SOL &\leq \frac{2\gamma Lsec\alpha}{L-(\sqrt{2}-1)\sqrt{C}} OPT_d + \kappa\gamma OPT_m \\ &\leq max\Big(\frac{2\gamma Lsec\alpha}{L-(\sqrt{2}-1)\sqrt{C}}, \kappa\gamma\Big) OPT \end{aligned} \tag{13}$$

which proves the theorem statement. □